7C.8 COHERENT STRUCTURES IN OCEAN SKIN TEMPERATURE VARIABILITY

Christopher J. Zappa*
Lamont-Doherty Earth Observatory, Columbia University, Palisades, NY

Andrew T. Jessup
Applied Physics Laboratory, University of Washington, Seattle, WA

J. Tom Farrar & Robert A. Weller
Woods Hole Oceanographic Institution, Woods Hole, MA

1. INTRODUCTION

Airborne infrared (IR) remote sensing techniques have been shown to quickly characterize the spatial and temporal scales of ocean skin temperature as well as a wide variety of processes that are important to the variability of air-sea fluxes of heat, mass, and momentum [*McAlister and McLeish*, 1965]. Results from Tropical Ocean-Global Atmosphere, Coupled Ocean-Atmosphere Response Experiment (TOGA-COARE) have demonstrated the importance of skin temperature in air-sea interaction. Accurate knowledge of the skin temperature has been shown to be critical to estimating surface fluxes [*Fairall et al.*, 1996b] and as a result its spatial variability influences the small-scale distribution of those fluxes [*Hagan et al.*, 1997; *Walsh et al.*, 1998]. The focus of our observations is the spatial variability of the ocean surface skin temperature under low wind conditions.

An early demonstration of the potential of IR imagery of the ocean surface from aircraft was reported by *McAlister and McLeish* [1965]. They performed some of the first measurements of the horizontal structure of ocean skin temperature using an IR scanner and recorded signatures of apparent fronts, large-scale ocean eddies, free-convective patterns, wind streaks, and whitecapping. However, there were no upper ocean measurements to corroborate the processes that occurred. *Peltzer et al.* [1987] used an airborne IR imaging system for the detection of ship wakes during the day, when the diurnal thermocline was well established. The thermal wake signatures recorded by the imaging system depict the contrast between the cool center of the ship wake produced by the upwelling of the underlying water and a warmer undisturbed surface layer. Smaller-scale process studies of ocean skin temperature have demonstrated the effect of deep-water breaking waves [*Jessup et al.*, 1997a], free-convective patchiness [*Zappa et al.*, 1998], microscale wave breaking [*Jessup et al.*, 1997b], and deep-water swell [*Jessup and Hesany*, 1996] on the ocean skin layer, which is often cooler than the underlying water [*Katsaros*, 1980b]. These measurements using IR imagery highlight a portion of the variety of processes that affect the ocean skin temperature.

Results using low-noise, high-resolution spatial series of skin temperature measured from aircraft during the 2001 CBLAST-Low Experiment in July-August [*Zappa and Jessup*, 2005] show that within the CBLAST-Low site it is characteristic to observe large-scale meridional and zonal temperature variability of 0.23°C km^{-1} and 0.27°C km^{-1}, respectively. Our analysis has demonstrated that this temperature variability results in meridional and zonal scalar heat flux variability of 7.0 W m^{-2} km^{-1} and 7.6 W m^{-2} km^{-1}, respectively.

The 2001 CBLAST-Low Experiment results also reveal a variety of mechanisms related to atmospheric and sub-surface phenomena that produce horizontal variability in ocean skin temperature over spatial scales ranging from *O*(10 km) down to *O*(1 m) under low to moderate wind conditions. Fine-scale maps of ocean surface temperature show a variety of processes including coherent ramp-like temperature structures and distinctive streaks of various scales. The IR imagery was compared with the subsurface temperature and velocity data from buoys. Internal wave and ramp-like mixing signatures were identified in the IR imagery and corroborated

* *Corresponding author address*: Christopher J. Zappa, Lamont-Doherty Earth Observatory, Columbia University, 61 Route 9W, Palisades, NY 10964; email: zappa@ldeo.columbia.edu

with the sub-surface data. These SST signatures were found to be sensitive to the interaction of the surface buoyancy forcing and mixing processes that spatially modulate the depth of the shallow oceanic mixed layer. These mixing processes may both support and result from the horizontal inhomogeneities in the upper ocean. The IR measurements themselves have provided important two-dimensional structure of the ocean surface features that may be missed by *in-situ* measurements. These fine-scale measurements demonstrate processes that directly affect the thermal boundary layer and therefore are important to upper-ocean mixing and transport dynamics as well as the magnitude and distribution of air-sea fluxes.

Here, we report on the spatial variability of ocean surface temperature using airborne infrared measurements during the field campaign of the Coupled Boundary Layers, Air-Sea Transfer in Low Winds (CBLAST-Low) Experiments in 2002 and 2003. The extensive spatial coverage and fine spatial and temperature resolution of our systems allows us to examine spatial scales in skin temperature from processes that span the atmospheric boundary layer of *O*(1km) down to wave-related processes *O*(1m). We produced thermal maps of the study site using time series of ocean skin temperature and compared these with the fine-scale structures observed within the IR imagery to investigate a variety of processes with varying scales in the coastal zone. We combine the airborne IR data with upper ocean measurements to relate horizontal variability in surface skin temperature to sub-surface phenomena.

2. CBLAST-LOW EXPERIMENTS

Measurements of ocean skin temperature variability were made during the main field campaigns of the CBLAST-Low (Coupled Boundary Layers, Air-Sea Transfer in Low Winds) experiment in August/September 2002 and July/August 2003 off the south coast of Martha's Vineyard. Central to the CBLAST-LOW site were the offshore tower [*Edson et al.*, 2004] and horizontal ocean buoy array [*Farrar et al.*, 2004]. We flew a state-of-the-art, high spatial resolution, dual up- and down-looking longwave IR imaging system that included in-flight calibration capability aboard a Cessna Skymaster shown in Figure 1. The surveys in 2002 and 2003 quantified the horizontal mesoscale variability in the domain around the CBLAST-LOW site near the offshore tower and the horizontal ocean mooring/buoy array throughout the region extending 40-50 km offshore.

Airborne measurements were made of horizontal variability of ocean surface skin temperature using two complimentary infrared (IR) sensors. An AIM model 640Q longwave infrared imager containing a 640 by 512 element QWIP focal-plane detector array sensitive to radiation in the 8-12 μm wavelength range provided high spatial and temporal resolution imagery. High-quality daytime measurements were achieved since the longwave detector minimized solar contamination of the IR imagery. A model KT-15 narrow field-of-view (FOV) radiometer (Heitronics, Wiesbaden, Germany) in the 8-14 μm wavelength range provided calibrated surface temperature at lower resolution. A sky correction was

Figure 1. (Top) Cessna Skymaster flown during CBLAST-LOW 2002/2003 based in Chatham, MA. (Bottom) Close-up of the downward-looking IR imager, collocated video camera, and collocated, narrow FOV IR radiometer.

implemented following [*Katsaros*, 1980a] with the corresponding upward-looking AIM imager and KT-15 radiometer. A downward-looking Pulnix model 9701 digital video camera (Pulnix America Inc., Sunnyvale, CA) was used to supplement these measurements. During each flight, the IR imagery was corrected for non-uniformity and calibrated using a model 2004S blackbody (Santa Barbara Infrared Inc., Santa Barbara, CA). The KT-15 radiometers were calibrated pre- and post-experiment in the laboratory, and provided an accurate measurement to compare directly with the calibrated AIM model 640Q imager measurements in-situ during flights.

The IR imager was operated concurrently in two distinct modes identified as Full Frame and Sub-Frame (Averaged) mode. Both modes obtain high spatial resolution and low noise temperature measurements. In the Full Frame mode, complete images were acquired at 1 Hz in order to provide an instantaneous 2-D map of surface temperature with a thermal resolution of roughly 0.02°C. For the nominal altitude of 610 m in 2002 and 875 m in 2003, the spatial resolution was less than 0.3 m and 0.9 m respectively. In the Sub-Frame mode, we sampled the IR imager at a fast frame rate (30 Hz) and then obtained a point measurement by taking the average of a subset of each image. Averaging of a subset of the 327,680 samples in each image reduced the noise and provided a high-resolution spot of the ocean surface. In this Sub-Frame mode, the imager provided a time/spatial series equivalent to a "spot" measurement of temperature with a temperature resolution of less than 0.02°C and a spatial resolution of *O*(1-10m) depending on the altitude and selected image subset matrix.

Operating the IR imager in Sub-Frame mode offers a noise level that is significantly below that for an IR radiometer at all spatial resolutions. For example, at the nominal altitude for the 2002 campaign of 610 m, the KT-15 radiometer had a temperature resolution of 0.2°C and a spatial resolution of 80 m compared to 0.03°C and 2.3 m respectively for the longwave IR imager.

3. TEMPERATURE VARIABILITY

During these IOP experiments, we observed remarkable variability in small-scale structures that suggests mechanisms related to subsurface phenomena that drive or enhance exchange. The 1-m resolution IR imagery shows high SST variability of several degrees on scales of *O*(10m – 1km) under a variety of wind speed conditions. The structure of this mean variability is evident in variance-preserving wavenumber spectra of the SST under conditions of very low wind to moderately high winds. Under low wind-speed conditions (0 to 2.5 m s^{-1}), the IR imagery shows high temperature variability on scales of *O*(1 m to 100 m) without the distinction of coherent structures. The spectra are characterized by a broad distribution of energy that decreases at high wavenumber with increasing wind speed. During one spectra at low wind, internal waves were present and a peak in the spectra occurred at a wavenumber of roughly 0.004 m^{-1}, that of the peak wavenumber for the internal waves. During moderate winds (2.5 to 5 m s^{-1}), the variability is on scales of *O*(100 m – 1 km) and is related to internal waves and coherent ramping structures. The spectra exhibit a significant energy drop at intermediate wavenumbers with a peak in wavenumber at roughly 0.01 m^{-1}, the scale of the coherent ramping structures. For wind speeds greater than 5 m s^{-1}, the data show significantly less temperature variability with incidence of breaking waves and distinct row/streak structures in the IR imagery that were aligned with the wind and were likely the surface manifestation of Langmuir circulation cells. Here, the energy in the spectra dips at intermediate wavenumbers but increase at higher wavenumber in the range 0.05 to 0.1 m^{-1}, the scales of observed Langmuir circulation. The wavenumber spectra in all wind-speed regimes are clearly affected and governed

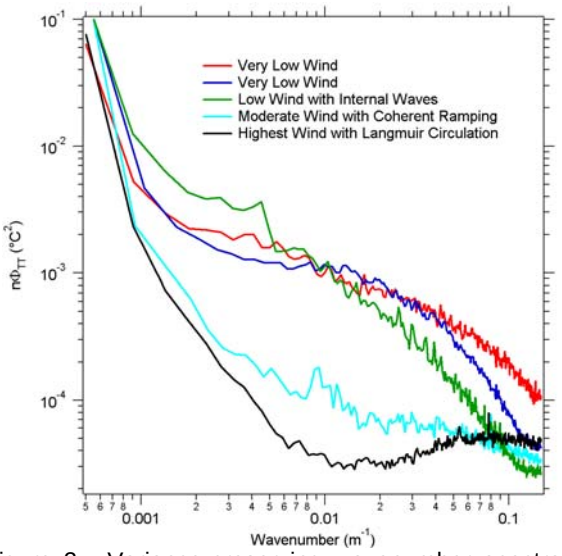

Figure 2. Variance-preserving wavenumber spectra of temperature from the infrared imagery for representative runs during the CBLAST-Low experiments of 2002 and 2003.

by the process within the near-surface ocean layer and/or the thermocline.

The data taken during CBLAST-Low in 2002 and 2003 in Figure 3 shows that the mean overall temperature variability decreases with wind speed. Figure 3 shows the mean skin temperature variability determined from the spectra in Figure 2 for the range of scales of 10 m to 1 km as a function of wind speed. The skin temperature variability clearly decreases with increasing wind speed and is related to mechanisms revealed in coherent structures of the IR imagery.

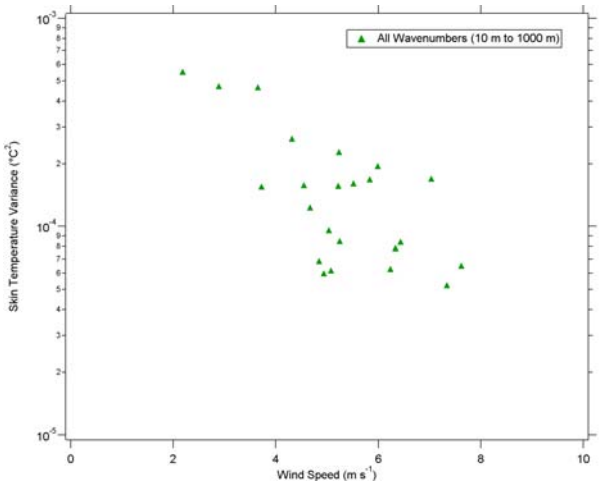

Figure 3. Mean skin temperature variance between 10 and 1000 m scales as a function of wind speed for each run during the CBLAST-Low experiments of 2002 and 2003.

4. INTERNAL WAVES

A case study on Aug 14, 2003 of coincident airborne SST and oceanic mooring data provides a clear example of the internal wave signature imprinted in the SST variability. Figure 4 shows a mosaic of the SST anomaly over 2 km directly over a heavy mooring site at 1946 UTC. The leading edge in the SST mosaic shows an increase in temperature followed by an abrupt decrease and subsequent return to ambient SST that is coincident with the passage of the internal wave in the subsurface temperature data. The SST mosaic suggests internal waves propagating onshore with crests oriented 45° from North. Current vectors during the time of the aircraft overpass associated with 30-minute period quasi-linear, energetic internal waves were observed at two nearby heavy moorings. As would be expected, the horizontal velocity signal of the internal waves is rectilinear and perpendicular to

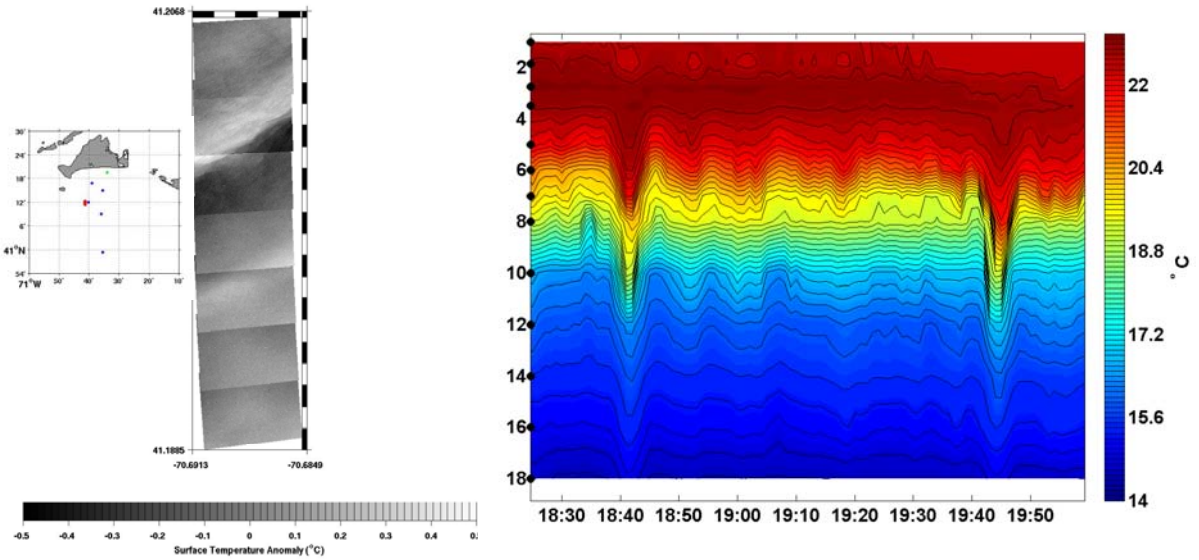

Figure 4. Mosaic (left) of SST anomaly over 2 km directly over a heavy mooring site at 1946 UTC Aug 14, 2003. Time series of temperature field (right) at the mooring site shows the internal waves propagating onshore. Current vectors associated with 30-minute period internal waves were observed at two nearby heavy moorings during the hour centered on the aircraft overpass. The internal wave crests in the SST signature are oriented perpendicular to the axis of the internal wave velocity fluctuations observed at the moorings. The inset shows the CBLAST-Low region. The red dot is the location of the aircraft, the blue dots are the mooring sites, and the green dot is the location of ASIT.

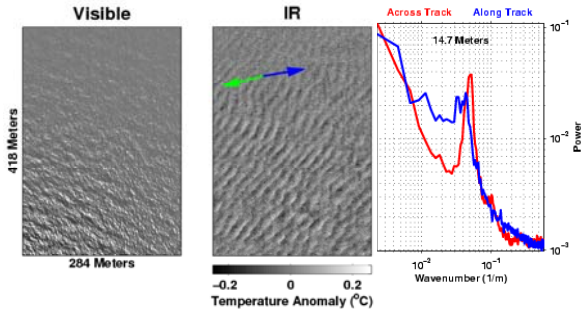

Figure 5. Visible image, IR image, and spectra of the IR image showing coherent ramp structures observed on August 14, 2003 in the afternoon. The wind speed (Blue Arrow) is roughly 4 m s^{-1} from the West and the surface current (Green Arrow) is 17 cm s^{-1} from the East. The variability in temperature across these coherent ramps is of O(0.5 ºC), their dominant scale is 14.7 m, and they extend over several km. The lack of coherent parallel features in the visible imagery suggests that the ocean surface features observed in the IR imagery are not related to surface gravity waves. Here, the skewness of the temperature variability is 2.8, strongly suggestive of "billows" from shear-induced turbulence.

the wave crest and trough signatures seen in the SST imagery.

Consistent with the observations of *Walsh et al.* [1998] and *Marmorino et al.* [2004], our analysis provides direct evidence that the SST spatial fluctuations are a surface expression of oceanic internal waves [*Farrar et al.*, 2004; *Farrar et al.*, 2006]. However, it is still unclear how the subsurface temperature signal is imprinted on the sea surface. *Walsh et al.* [1998] hypothesized that the SST signal was caused by internal wave modulation of near surface mixing, while *Marmorino et al.* [2004] hypothesized that the SST signal was a result of vertical straining of the aqueous thermal boundary layer by the internal waves. Either mechanism may dominate for a given condition. Analysis is proceeding under the hypothesis that the surface signal is due to a combination of near surface mixing, which may directly imprint the signal on the surface, and the surface vertical strain associated with the waves, which may modify the magnitude of the cool skin effect [*Farrar et al.*, 2006].

5. RAMP-LIKE STRUCTURES

Fine-scale imagery of ocean skin temperature elucidated a variety of mechanisms related to atmospheric and sub-surface phenomena that produce horizontal variability over a wide range of scales. In particular, we observed extensive regions (*O*(1 km)) with embedded sharp coherent temperature ramps of *O*(0.5ºC) with spacing of *O*(10 m) (see Figure 5) during moderate winds (2.5 to 5 m s^{-1}). These coherent ramp structures may be the IR signature of a mechanism in the near-surface layer that leads to the stratification breakdown as the wind-driven shear erodes the near-surface stratification that was established during the peak daytime heating. The dominant spatial scale of the variability in temperature across these coherent ramps is 14.7 m, and they extend over several km. The lack of coherent parallel features in the visible imagery suggests that the ocean surface features observed in the IR imagery are not related to surface gravity waves [*Jessup and Hesany*, 1996]. A warm layer model [*Fairall et al.*, 1996a], commonly used to predict the evolution of temperature very near the surface, suggests that shear instabilities are likely during this time. *Thorpe* [1988] observed similar coherent structures during stable stratification that exhibited positive skewness. Here, the observed skewness is 2.8, which is significantly greater than that observed by *Thorpe* [1988] and strongly suggestive of "billows" due to shear-induced instability.

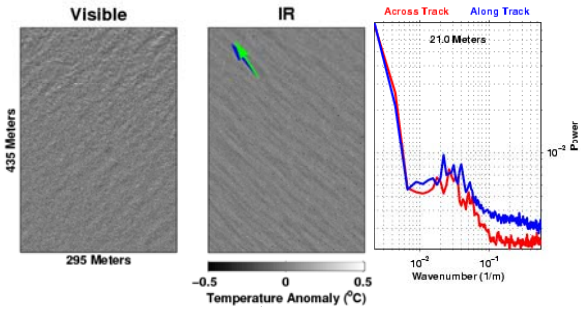

Figure 6. Video image, IR image, and spectra of the IR image depicting Langmuir circulation observed on August 25, 2003 in the morning. The wind speed (Blue Arrow) is roughly 5 m s^{-1} and the surface current (Green Arrow) is 47 cm s^{-1}, both from the West-SouthWest. The IR image shows an ocean surface with thin bands of cool water that are parallel to the wind and about 0.2°C less than the regions between the bands. The dominant scale between these cool bands is 21.0 m, the features are evident throughout the CBLAST-Low region, and the temperature variability is calculated to be Gaussian. These parallel-aligned structures with the wind and perpendicular to the waves in the video are suggestive of Langmuir circulation.

6. LANGMUIR CIRCULATION

For wind speeds greater than 5 m s^{-1}, there is significantly less spatial variability in SST, but we observe distinct row/streak structures aligned with the wind. These features are likely due to Langmuir circulation cells (Figure 6). The horizontal spacing of these features coincided with wind-aligned surface slicks and bubbles visible in the video. The wind speed in Figure 6 is roughly 5 m s^{-1} and the surface current is 47 cm s^{-1}, both from the west-southwest. The IR image shows an ocean surface with thin bands of cool water that are parallel to the wind and about 0.2°C less than the regions between the bands. The dominant scale between these cool bands is 21.0 m, the features are evident throughout the CBLAST-Low region, and the distribution of temperature variability is approximately Gaussian. The combination of a well-mixed layer with the wind and wave orientation seen in Figure 6 provides a highly favorable environment for the development of Langmuir circulation. These structures, aligned with the wind and perpendicular to the surface waves, are suggestive of Langmuir circulation. In addition, the spacing of the cells agrees well with the scale expected for Langmuir cells, given the approximately 6 m deep mixed layer observed at the moorings. These fine-scale measurements demonstrate processes that directly affect the thermal boundary layer and therefore are important to upper-ocean mixing and transport dynamics as well as the magnitude and distribution of air-sea fluxes.

7. DISTRIBUTIONS OF LENGTH SCALES

The distribution of length scales has been investigated by determining the dominant scale for individual IR images during CBLAST-Low 2003. Length scales are determined from individual images using an algorithm developed during this year that couples Radon Transform and FFT methodologies. Differences in the distributions are associated with different features. Figure 7 shows the distributions of length scales from three flights that were dominated by different features including coherent ramping structures (Top; as in Figure 5), coherent ramping structures within an active internal wave field (Middle), and Langmuir circulation (Bottom; as in Figure 6). The left graph in each is the distribution of length scales. Notice that the distribution of length scales for both the coherent ramping structures alone and Langmuir circulation are similarly weighted toward smaller scales less than 25 m. This is not surprising since the observed scales in Figures 5 and 6 are comparable. However, Langmuir circulation signatures are more prevalent. The comparable distributions for two distinct mechanisms suggest that another controlling factor such as depth may be important. However, the active internal wave field significantly modulates the coherent ramping structures causing the distribution to be weighted toward larger scales greater than 25 m as well as more instances of coherent

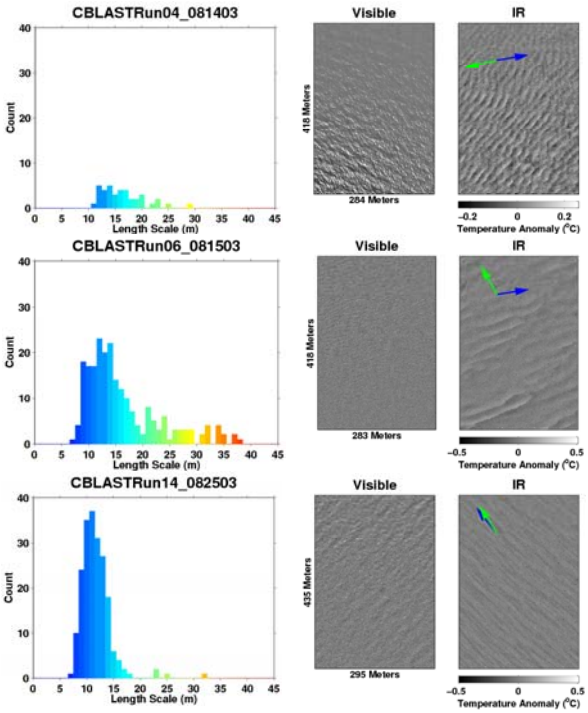

Figure 7. Distributions of length scales (Left plot in each pair) determined from individual IR images using the Radon processing method during CBLAST-Low 2003 for examples of coherent ramping structures (Top), coherent ramping structures within an active internal wave field (Middle) and Langmuir circulation (Bottom). On the right show the visible and IR imagery corresponding to the signature defining the distribution on the left.

structures. This suggests that the larger internal wave packets trigger smaller-scale disturbances within the near-surface layer.

8. ACKNOWLEDGEMENTS

The authors would like to thank Jim Edson for his instrumental effort in making CBLAST-Low a reality and for providing the ASIT meteorological data used in this study. Felix Tubiana performed much of the IR imagery data analysis. The authors are grateful to the Office of Naval Research for support of this work through the CBLAST-LOW DRI.

9. REFERENCES

Edson, J.B., F. Crofoot, W.R. McGillis, and C.J. Zappa, Investigations of flux-profile relationships in the marine atmospheric

surface layer during CBLAST, in *16th Symposium on Boundary Layers and Turbulence*, Ref. 8.2, Portland, Maine, USA, 2004.

Fairall, C.W., E.F. Bradley, J.S. Godfrey, G.A. Wick, J.B. Edson, and G.S. Young (1996a), Cool-skin and warm-layer effects on sea surface temperature, *J. Geophys. Res.*, *101* (C1), 1295-1308.

Fairall, C.W., E.F. Bradley, D.P. Rogers, J.B. Edson, and G.S. Young (1996b), Bulk parameterization of air-sea fluxes for Tropical Ocean Global Atmosphere Coupled Ocean Atmosphere Response Experiment, *J. Geophys. Res.*, *101* (C2), 3747-3764.

Farrar, J.T., R.A. Weller, C.J. Zappa, and A.T. Jessup, Subsurface expressions of sea surface temperature variability under low winds, in *16th Symposium on Boundary Layers and Turbulence*, Ref. P8.1, Portland, Maine, USA, 2004.

Farrar, J.T., C.J. Zappa, R.A. Weller, and A.T. Jessup, Sea surface temperature signatures of oceanic internal waves in low winds, in *27th Conference on Hurricanes and Tropical Meteorology*, Ref. P11.2, Monterey, California, USA, 2006.

Hagan, D., D. Rogers, C. Friehe, R. Weller, and E. Walsh (1997), Aircraft observations of sea surface temperature variability in the tropical pacific, *J. Geophys. Res.*, *102* (C7), 15733-15747.

Jessup, A.T., and V. Hesany (1996), Modulation of ocean skin temperature by swell waves, *J. Geophys. Res.*, *101* (C3), 6501-6511.

Jessup, A.T., C.J. Zappa, M.R. Loewen, and V. Hesany (1997a), Infrared remote sensing of breaking waves, *Nature*, *385* (6611), 52-55.

Jessup, A.T., C.J. Zappa, and H. Yeh (1997b), Defining and quantifying microscale wave breaking with infrared imagery, *J. Geophys. Res.*, *102* (C10), 23145-23153.

Katsaros, K., Radiative sensing of sea surface temperature, in *Air Sea Interaction: Instruments and Methods*, edited by F. Dobson, L. Hasse, and R. Davis, pp. 293-317, Plenum Press, New York, 1980a.

Katsaros, K.B. (1980b), The aqueous thermal boundary layer, *Boundary-Layer Meteorology*, *18*, 107-127.

Marmorino, G.O., G.B. Smith, and G.J. Lindemann (2004), Infrared imagery of ocean internal waves, *Geophys. Res. Lett.*, *31* (11), L11309, doi:10.1029/2004GL020152.

McAlister, E.D., and W.L. McLeish, Oceanographic measurements with airborne infrared equipment and their limitations, in *Oceanography From Space*, edited by G.C. Ewing, pp. 189-215, Woods Hole Oceanographic Inst. Rep. No. 65-10, Woods Hole, MA, 1965.

Peltzer, R.D., W.D. Garrett, and P.M. Smith (1987), A remote sensing study of a surface ship wake, *Int. J. Remote Sensing*, *8* (5), 689-704.

Thorpe, S.A. (1988), The dynamics of the boundary layers of the deep ocean, *Science Progress*, *72* (286), 189-206.

Walsh, E.J., R. Pinkel, D.E. Hagan, R.A. Weller, C.W. Fairall, D.P. Rogers, S.P. Burns, and M. Baumgartner (1998), Coupling of internal waves on the main thermocline to the diurnal surface layer and sea surface temperature during the Tropical Ocean-Global Atmosphere Coupled Ocean-Atmosphere Response Experiment, *J. Geophys. Res.*, *103* (C6), 12613-12628.

Zappa, C.J., and A.T. Jessup (2005), High resolution airborne infrared measurements of ocean skin temperature, *Geoscience and Remote Sensing Letters*, *2* (2), doi:10.1109/LGRS.2004.841629.

Zappa, C.J., A.T. Jessup, and H.H. Yeh (1998), Skin-layer recovery of free-surface wakes: Relationship to surface renewal and dependence on heat flux and background turbulence, *J. Geophys. Res.*, *103* (C10), 21711–21722.